Stability of PEDOT:PSS-Coated Gold Electrodes in Cell Culture Conditions

Gerwin Dijk[+] *and Alexandra L. Rutz*[+]*, George G. Malliaras**

[+] shared first author-ship

G. Dijk
Department of Bioelectronics, Ecole Nationale Supérieure des Mines, CMP-EMSE, 13541 Gardanne, France
Panaxium SAS, 13100 Aix-en-Provence, France
Dr. A. L. Rutz, Prof. G. G. Malliaras
Electrical Engineering Division, Department of Engineering, University of Cambridge, 9 JJ Thomson Ave, Cambridge CB3 0FA, UK
E-mail: gm603@cam.ac.uk

Keywords: conducting polymers, electrophysiology, electrodes, PEDOT:PSS, microelectrode array

Abstract

Poly(3,4-ethylenedioxythiophene) doped with polystyrene sulfonate (PEDOT:PSS) is widely used as a coating on microelectrode arrays in order to reduce impedance for both *in vitro* and *in vivo* electrophysiology. In many applications, electrode performance of months to years is desired; yet, there are few studies to date that examine the long-term stability of conducting polymers and their devices. Here, the stability of PEDOT:PSS microelectrodes is examined over a period of four months in cell culture media enriched with fetal bovine serum. The electrochemical impedance remains constant for most electrodes throughout the study, and only small changes in the structure of functional electrodes are observed at the end of the test. The results demonstrate that PEDOT:PSS electrodes show adequate stability for a variety of *in vitro* electrophysiology applications in toxicology, drug development, tissue engineering, and fundamental studies of electrically active cells and tissues.

Electrophysiology involves the use of electrodes for recording and stimulation of cells and tissues. *In vitro*,[1] electrophysiology is used for drug development and toxicity studies, as

well as in tissue engineering and developmental biology. *In vivo*, electrodes are used to study the central nervous system as well as in clinical diagnosis, brain-computer interfaces and function restoration after disease or injury to the nervous system.[2] In order to improve recording and stimulation, metal electrodes can be coated with conducting polymers[3–5] that decrease impedance by increasing the effective area for ionic-electronic transduction.[6,7] These coatings permit the development of arrays comprising smaller electrodes placed at a higher density, and hence, improve the spatial resolution of electrophysiology.[8]

Poly(3,4-ethylenedioxythiophene) doped with polystyrene sulfonate (PEDOT:PSS) has been established as the champion material for electrophysiology due to its low impedance, cytocompatibility, and commercial availability.[6,9,10] PEDOT:PSS has demonstrated excellent short-term (weeks) stability; yet, there are limited works exploring long-term performance.[16,17,20][18][19][21][22] Many electrophysiological applications, however, require long-term usage including cell culture on microelectrode arrays for recording and stimulation,[11,12] which can last several months, as well as in implantable devices that often need to remain viable for the lifetime of the patient.[13] Physiological conditions expose electrodes to complex aqueous solutions (cell culture media or extracellular fluid in tissues) containing species such as ions, proteins, and sugars. Furthermore, as a consequence of the foreign body response to implantable devices, inflamed tissue can also produce reactive oxygen species.[14] Thus, towards developing conducting polymer-based electrophysiology devices that can last years, it is important to understand how electrodes perform in such conditions as well as what failures occur and at what frequency.[15]

In the context of stimulation, PEDOT:PSS-coated electrode stability has been shown to be dependent on operating parameters as well as coating thickness. Stable electrode performance has been reported at rest (no stimulation applied),[16,17] but electrodes have failed (e.g. high impedance, cracking, delamination) with thicker PEDOT:PSS coatings.[18] Successful strategies for active electrode durability include promoting polymer-substrate

adhesion with nanostructured platinum and iridium oxide.[19] For recording, only a small number studies to date have explored the stability of PEDOT:PSS for more than a few weeks.[16,17,20][21][22] Generally, stable impedances or marginal increases (<10%) have been reported *in vitro* in buffered saline solutions (phosphate buffered saline or artificial cerebro-spinal fluid) for PEDOT:PSS coatings that were deposited on metal electrodes using electrochemical polymerization.[16,17,20] However, after implantation in the brains of rodents[16,20,21] and non-human primates,[22] higher impedance increases have been reported. Especially in the first week, an increase of nearly one order of magnitude was observed but was then followed by a stable impedance.[16,21] Biofouling from proteins in the extracellular fluid as well as binding of cells as part of the foreign body response have been hypothesized as potential causes. However, the *in vivo* environment is highly complex, and there are many other possible failure mechanisms that could account for the differences between *in vitro* and *in vivo* results. Therefore, further investigation is needed to independently study hypothesized failure mechanisms.

In this manuscript, we added further complexity to the incubating media by using standard cell culture media containing 10% fetal bovine serum and therefore, introduced the possibility of protein biofouling. Moreover, we use PEDOT:PSS that is deposited using spin coating from a commercial dispersion after addition of a crosslinker, a process that is consistent with large-scale manufacturing. Recently, this material formulation has demonstrated viability for clinical translation in first-in-human studies.[8,23] To the best of our knowledge, no one has reported on the long-term performance of these solution-deposited PEDOT:PSS electrodes, despite their manufacturability and clinical relevance.

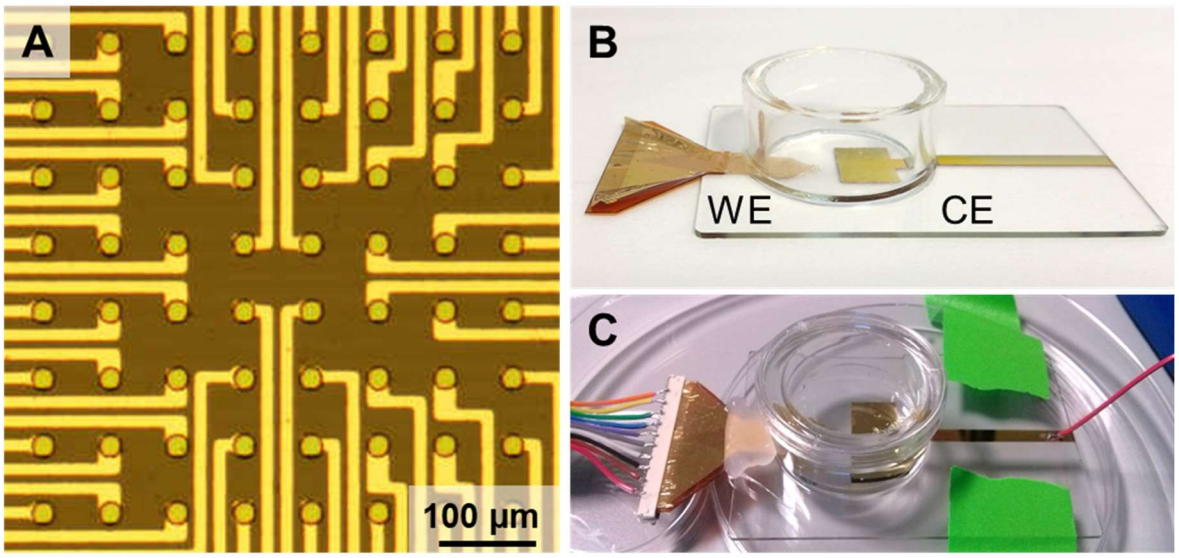

Figure 1. Experimental set-up for sterile electrochemical impedance spectroscopy (EIS). A) Microfabricated electrode array composed of 64 PEDOT:PSS-coated gold electrodes with 20 µm diameter. Electrode array is embedded in parylene C. B) Electrode array (working electrode, WE) glued to a glass slide with a large PEDOT:PSS-coated gold electrode (1 x 1.5 cm) serving as the counter electrode (CE). A silicone well was placed on top in order to confine the media around each. The three components adhered together were autoclaved for sterility. C) A sterile petri dish lid was fitted on the silicone well to maintain sterility with a closed system. The electrode array device was connected with a ZIF clip, soldered with wires for connection. The gold CE was also soldered with a wire. The entire set-up was incubated in a cell culture incubator and was removed for EIS timepoints.

The stability of PEDOT:PSS-coated electrodes was investigated by performing electrochemical impedance spectroscopy (EIS) over the four-month incubation period in cell culture media. EIS is commonly used to determine electrode impedance, a measure that predicts the potential for high quality biological recordings. Importantly, EIS is performed with small voltages (10 mV) and therefore, the measurements do not have a substantial effect on the electrodes. The electrodes were part of a flexible array fabricated on parylene C with standard microfabrication processes as reported elsewhere.[24] The array contained 64 gold electrodes with a diameter of 20 µm and coated with the PEDOT:PSS dispersion (**Figure 1**a).

Incubation in cell culture media necessitated sterility in order to avoid bacterial or fungal growth that could confound results. Significant bacterial and fungal biofouling would not be observed in typical *in vitro* or *in vivo* applications. Therefore, we needed to develop a set-up for sterile and stable EIS. Introducing external electrodes (e.g. Ag/AgCl, Pt) into the

electrolyte for EIS created a source of potential contamination. Instead, a permanent counter electrode was incorporated. The set-up consisted of a glass substrate with a large gold counter electrode, CE, and the microelectrode array (working electrode, WE) was glued in place near it. In this two-electrode configuration, the CE was almost half a million times larger than the WE, ensuring that all the applied potential dropped at the WE/electrolyte interface. A silicone well was fixed onto the glass substrate to confine the media and immerse all electrodes (Figure 1b). Furthermore, the set-up was designed while considering sterilization methods. These components brought together are all compatible with steam autoclave, a clinically used sterilization method. Previous work has shown that autoclaving PEDOT:PSS electrodes has little impact on electrical properties.[25]

Immediately after autoclaving, a sterile petri dish lid was fitted on top of the well to establish a closed system that ensures sterility. Finally, in order to have stable and quick connections throughout the study, the CE electrode was soldered with a wire, and the electrode array was connected to a zero insertion force (ZIF) clip soldered with 10 wires (Figure 1c). Ten of the 64 electrodes were randomly chosen for EIS measurements based on the ZIF clip connection. This complete set-up was incubated in cell culture conditions (37 °C and 5% CO_2) and was only removed to perform EIS and to refresh media. While some studies have utilized standard protocols[26] for accelerated aging by incubating devices at higher temperatures, physiological temperature was used here in order to avoid protein denaturation that could impact the nature of electrode fouling. Additionally, the conditions used here were identical to the ones used in *in vitro* electrophysiology, hence relevant to applications. All EIS measurements were conducted in cell culture media, and it was found that the spectrum did not greatly differ from the spectrum in phosphate-buffered saline solution (Figure S1). Before EIS testing, the electrode array was washed with deionized water to remove excess PSS^- and any low molecular weight compounds for stable baseline impedance measurement.

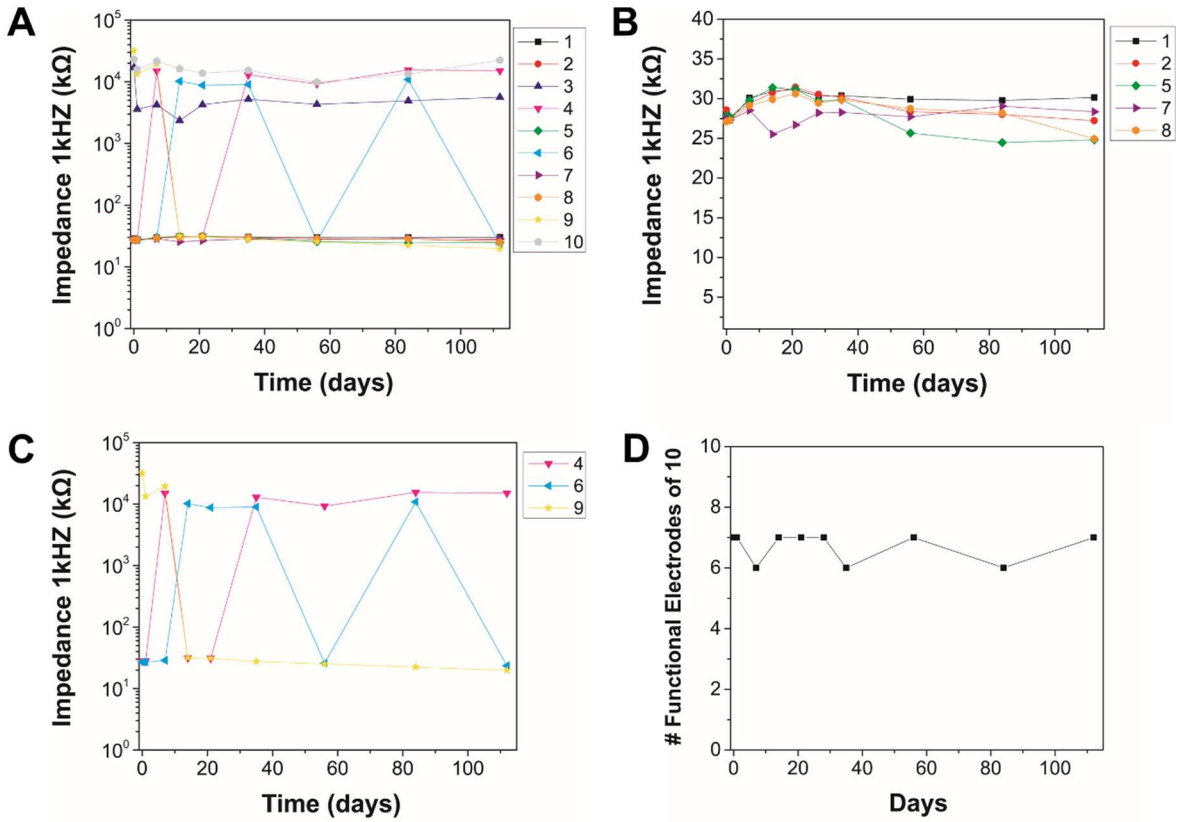

Figure 2. Expected functionality analysis of individual electrodes (N=10) with time. Numbers correspond to different electrodes. Functional electrodes defined as those < 1 MΩ at 1 kHz. Three of the selected electrodes were non-functional at fabrication; two of these remained so throughout study period while one electrode became functional. Two electrodes varied between functional and non-functional throughout the study. A) all electrodes (10 in total) studied. B) only electrodes with good and stable performance (5 in total). C) only electrodes with variable functionality (3 in total). D) The number of functional electrodes over the course of the study. At any given timepoint, 6 to 7 of the 10 selected electrodes were functional.

The variation of electrode functionality with time was studied by examining the impedance at 1 kHz, the frequency corresponding to recordings of individual action potentials (single units) (**Figure 2,** Figure S2). "Functional" electrodes were defined as those with an impedance less than 1 MΩ at 1 kHz and "non-functional" electrodes as those with any higher impedance values. Although this impedance threshold is generally regarded as a marker of electrode functionality, some have reported this is not always the case.[27,28] At the beginning of the study, seven of the ten selected electrodes were functional and had an average

impedance of 27.8 kΩ ± 0.6 at 1 kHz (Figure 2a). Five of these seven electrodes (1, 2, 5, 7, 8) were functional throughout the entire period and showed low and stable impedance (25.5 kΩ ± 3.4 average impedance at 1 kHz at day 112; Figure 2b). After day 35, electrodes began to show slightly more variation in impedance. Interestingly, one of the non-functional electrodes became functional early in the study at day 14 and remained so for the rest of the period (electrode 9, Figure 2c). The other two non-functional electrodes (3 and 10) were non-functional from the start and remained so throughout the entire experiment. Two electrodes (4 and 6) fluctuated between functional and non-functional (Figure 2c). When high impedances were observed, we ensured that there was no debris on top of the electrodes by forcefully pipetting the media to generate flow and observed the same impedance again. These impedance fluctuations, referred to as 'blinking', have been reported before by others, *in vitro*[29] and when implanted in the brain.[30] Altogether, at any given timepoint 6 to 7 of the 10 electrodes were functional (Figure 2d).

The impedance spectra of functional and non-functional electrodes was compared to that of a bare gold (no PEDOT:PSS) electrode and that of an open circuit (working electrode disconnected) to look for delamination and connection failures, respectively (Figure S2a). A functional, PEDOT:PSS-coated electrode displayed a typical spectra consisting of a relatively flat, resistance-dominated region and a negatively sloped, capacitance-dominated region.[31] A gold electrode of the same diameter had a higher impedance that was capacitance dominated. The open circuit spectra showed higher impedance than the gold electrode, and furthermore, displayed erratic impedance values at 100 Hz and below. By examining each individual electrode, all non-functional EIS measurements matched that of the open circuit configuration. Therefore, we believe when electrodes were non-functional, including at the start or later in the study, that this was due to connection issues. More specifically, we believe these connection issues arose at the ZIF clip-parylene device interface. Manual alignment between ZIF clip pins and device contact pads as well as these rigid pins exerting significant

pressure on a thin, flexible substrate could have caused poor contact. Reliable connections for flexible devices remain a pressing challenge in the field, and from our experience here, we suggest chemical bonding, instead of mechanical means, as well as the use of alignment tools and automated processes to improve this aspect.

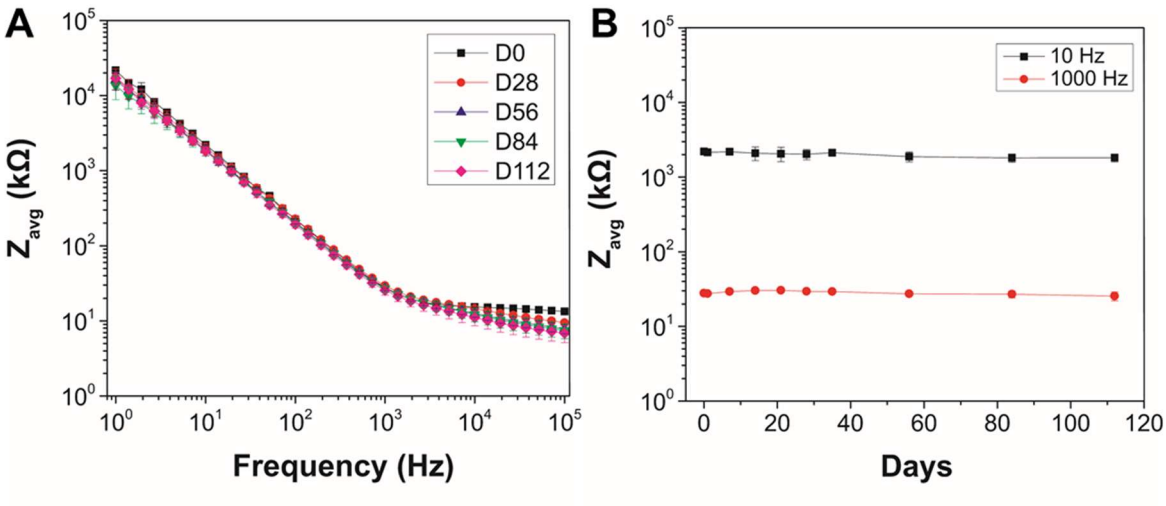

Figure 3. Impedance analysis with time of all functional electrodes. A) Average impedance spectra with standard deviations for all functional electrodes at the start of the study as well as each month, 1-4. B) Average impedance of functional electrodes with respect to time with standard deviations. Slight decreases in impedance were observed at mid (1000 Hz) and low (10) frequencies, corresponding frequencies of action potential (single-unit) and local field potentials, respectively.

The long-term behavior of the functional electrodes was further evaluated by examining the average impedance spectrum (**Figure 3**a). Generally, neural electrophysiological recordings are performed for capturing local field potentials and single action potential activity, which correspond to 10 Hz and 1000 Hz frequencies, respectively. At both frequencies, impedance of functional electrodes slightly varied with time (typically 5-10% of the initial value) (Figure 3b). Slight impedance increases at 1000 Hz were observed up until day 21 when the average impedance was approximately 9% higher than the initial value. After day 21, the impedance began to decrease for the remaining period. The final (day 112) average impedance values of functional electrodes were approximately 17% and 8%

lower than the initial value at 10 Hz and 1000 Hz, respectively. Finally, the small standard deviations among the functional electrodes indicated homogeneous properties.

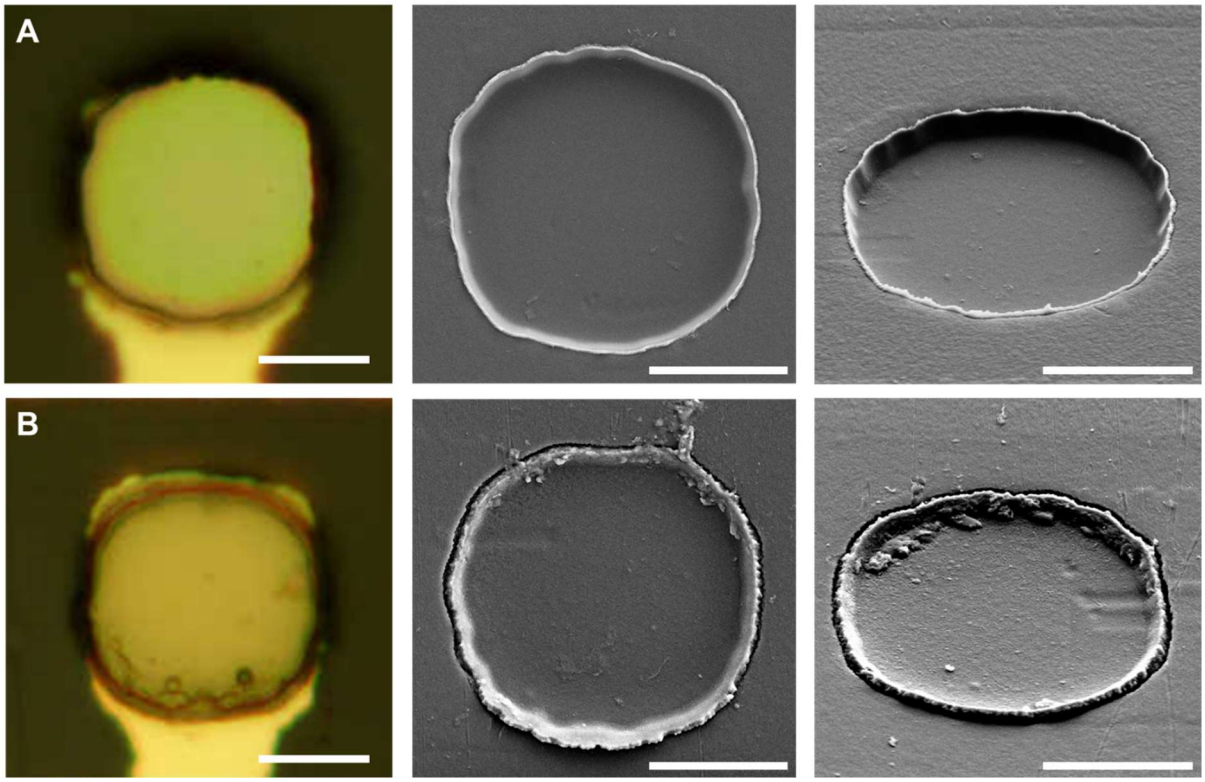

Figure 4. Imaging of A) as-fabricated electrode, before culture study and B) aged electrodes (functional). Left, optical images of electrodes. PEDOT:PSS showed a slight difference in color and some changes at the edges. Middle and right, scanning electron micrographs. The surface of the aged electrode appeared to have greater roughness and there was unknown debris in one part of the periphery. The aged PEDOT:PSS also appeared to be have increased in volume. Scale bars 10 µm.

After four months of incubation, the electrode array was washed with deionized water and dried, and all of the 64 electrodes were examined by optical microscopy and scanning electron microscopy (SEM) (**Figure 4,** Figure S3-5). For comparison, images of an electrode directly after fabrication were taken as well. Forty-six out of the 64 electrodes (>70%) showed no visible signs of degradation, and these include the impedance-fluctuating electrodes (4, 6, 9). The PEDOT:PSS material was intact and covered the entire electrode area. Furthermore, nearly all of the examined surface area of the parylene C encapsulation did not show any apparent damage (Figure S3a).

Of the electrodes that showed damage, four showed partial delamination of cracked PEDOT:PSS (Figure S3, S5). Delamination of PEDOT:PSS electrodes has been reported before.[18] Delamination is especially believed to be a consequence of poor material binding between the conducting polymer and underlying substrate,[32] and therefore, physical[19,33] and chemical[34] means of adhesion are recommended. In our case, we have used GOPS as a cross-linker[35] of the PEDOT:PSS and to help with substrate adhesion; although, it is not expected that there is chemical bonding between this polymer and metal.

Observed by light microscopy, the color of three electrodes changed considerably (Figure S3a). One electrode showed a ruptured PEDOT:PSS-parylene C interface (Figure S5), and one electrode showed some sort of PEDOT:PSS corrosion (Figure S4). Finally, nine electrodes appeared to have lost one of the two layers of deposited PEDOT:PSS as determined by light and scanning electron microscopy (Figure S3, S5). These material failures were clustered in the central part of the array, and thus, could be due to flaws from the fabrication process like contamination or inhomogeneous oxygen plasma treatment (Figure S3).

A potential fragile aspect of the electrodes is the PEDOT:PSS-parylene C interface, where we observed slight separation between the materials, especially for the discolored electrodes (Figure S4-S5). Such material separation could become a point of failure in longer-term studies of years. However, it should be noted that the SEM of the electrodes captures their dry state. Thus, during device operation in aqueous conditions and significant PEDOT:PSS swelling,[36] it is unclear whether or not this separation would be present.

Among the functional electrodes (1, 2, 5, 7, 8), as determined by EIS above, there were no major signs of damage but a couple subtle differences were observed (Figure 4, Figure S4). The aged electrodes appeared to have a slightly darker color, and the PEDOT:PSS coatings seemed to have increased in volume as well as surface roughness. Also, there are indications of some debris, visible along the periphery of the electrodes. Despite these slight

differences, none of these visible changes had influenced electrical properties. Aside from electrode 3, which showed delamination of the first PEDOT:PSS layer, the unstable (4, 6, 9) and non-functional (10) electrodes did not show any apparent signs of material damage, which supports our conclusions that non-functional electrodes were mostly due to connection issues (Figure S4).

In conclusion, we demonstrated that PEDOT:PSS-coated gold electrodes were largely stable in cell culture conditions for at least four months. When high impedance values were recorded (non-functional), connection issues were determined to be the main cause. To the best of our knowledge, this is the first report on the long-term stability of PEDOT:PSS electrodes prepared from solution using a scalable manufacturing technique. These results are of consequence to *in vitro* electrophysiology for toxicology, drug development, tissue engineering, and fundamental studies of electrically active cells and tissues. Such electrodes will be useful for long-term electrophysiology of cell and tissue cultures. The presence of cells *in vitro* is not expected to drastically change the results found here. These results are also promising regarding the potential of these electrodes for chronic use in implantable medical devices.

Experimental Section

Array Fabrication: The fabrication of the electrode array has been reported elsewhere.[24] Briefly, 2 µm parylene C was deposited by a SCS Labcoater 2 on a clean glass slide. Metal electrodes and connection leads were patterned using a lift-off process with a bi-layer of LOR5A resist and S1813 photoresist. Photoresist was exposed with a SUSS MBJ4 contact aligner. An adhesion layer of 10 nm chromium and 150 nm of gold was evaporated with a Boc Edwards thermal evaporator. After lift-off, a 2 µm parylene C insulation layer was

deposited with 3-(trimethoxysilyl)propyl methacrylate (A-174 Silane) as an adhesion promotor. The outline of the probe was etched with an Oxford Plasmalab 80 Plus (reactive ion etcher) using lithographically patterned AZ9260. The electrodes were coated with PEDOT:PSS by the following process. A soap layer was spin-coated before the deposition of a 2 μm sacrificial layer of parylene C. AZ9260 was spin coated, exposed and developed with AZ developer and subsequently, the parylene C was etched. A mixture of Heraeus Clevios PH1000 (aqueous colloidal dispersion of chemically polymerized PEDOT:PSS), ethylene glycol, dodecyl benzene sulfonic acid and (3-glycidyloxypropyl) trimethoxysilane was spin-coated two times (3000 rpm and 1500 rpm) with a one minute bake in-between at 110 °C. The sacrificial parylene C layers were peeled-off followed by a one hour bake at 140 °C. Finally, the device was washed in deionized water to remove excess low molecular weight compounds and to delaminate the device from the glass slide.

Set-up Assembly: A gold counter electrode (CE, 1 x 1.5 cm) was patterned on the glass substrate by using a polyimide foil mask and thermal evaporation of chromium and gold (10 nm and 150 nm, respectively). The CE was coated with the same PEDOT:PSS formulation as the electrodes of the array to minimize the CE/electrolyte voltage drop. The flexible electrode array was supported by polyimide foil except at the tip. The electrodes were at the tip of the array and the tip was glued near the counter/reference electrode to keep it in place throughout the experiment. The silicone well was secured to the glass by gluing it with polydimethylsiloxane (PDMS, Dow Corning Sylgard 184). After sterilization, a wire was soldered to the counter/reference electrode, and wires were soldered to a zero insertion force (ZIF) clip that was connected to the electrode array.

Array Sterilization and Incubation: The array, large gold electrode, and silicone well (PDMS, Dow Corning Sylgard 184) were sterilized by steam autoclave for 20 min at 121 °C and 220 kPa (no dry time). Media (Dulbecco's Modified Eagle Medium with phenol red and

10% fetal bovine serum) was refreshed once or twice weekly in a cell culture hood with aseptic technique. The device was incubated at 37 °C/ 5% CO_2 at all times, except for EIS.

Electrochemical Impedance Spectroscopy: EIS measurements were performed with an Autolab PGSTAT128N where the PEDOT:PSS-coated electrodes from the array were the working electrodes and the large 1 x 1.5 cm electrode was the counter electrode. A 10 mV sinusoidal voltage was applied at a frequency range of 1 Hz to 100,000 Hz.

Scanning Electron Microscopy: Scanning electron micrographs of the electrode array were acquired with a Carl Zeiss Ultra 55 after depositing 5 nm of gold-palladium on the electrode array with a Gatan 682 Precision Etching and Coating System (PECS).

Supporting Information
Supporting Information is available from the Wiley Online Library or from the author.

Acknowledgements
G.D. and A.L.R. contributed equally to this work. A.L.R. acknowledges support from the Whitaker International Scholars Program and the European Commission's Horizon 2020 Marie Sklodowska-Curie Individual Fellowship BRAIN CAMO (No. 797506). G.D. acknowledges support from the European Commission through the project of OrgBIO-ITN 607896.

Received: ((will be filled in by the editorial staff))
Revised: ((will be filled in by the editorial staff))
Published online: ((will be filled in by the editorial staff))

References

[1] M. E. Spira, A. Hai, *Nat. Nanotechnol.* **2013**, *8*, 83.

[2] R. Chen, A. Canales, P. Anikeeva, *Nat. Rev. Mater.* **2017**, *2*, 16093.

[3] S. Ghosh, O. Inganäs, *Adv. Mater.* **1999**, *11*, 1214.

[4] X. Cui, V. a Lee, Y. Raphael, J. a Wiler, J. F. Hetke, D. J. Anderson, D. C. Martin, *J. Biomed. Mater. Res.* **2001**, 261.

[5] X. Cui, J. F. Hetke, J. a Wiler, D. J. Anderson, D. C. Martin, *Sensors and actuators* **2001**, *93*, 8.

[6] E. Zeglio, A. L. Rutz, T. E. Winkler, G. G. Malliaras, A. Herland, *Adv. Mater.* **2019**, *31*, 1806712.

[7] D. C. Martin, G. G. Malliaras, *ChemElectroChem* **2016**, *3*, 686.

[8] D. Khodagholy, J. N. Gelinas, T. Thesen, W. Doyle, O. Devinsky, G. G. Malliaras, G. Buzsáki, *Nat. Neurosci.* **2015**, *18*, 310.

[9] D. T. Simon, E. O. Gabrielsson, K. Tybrandt, M. Berggren, *Chem. Rev.* **2016**, *116*, 13009.

[10] S. Inal, J. Rivnay, A. O. Suiu, G. G. Malliaras, I. McCulloch, *Acc. Chem. Res.* **2018**, *51*, 1368.

[11] W. Gong, J. Sencar, D. J. Bakkum, D. Jäckel, M. E. J. Obien, M. Radivojevic, A. R. Hierlemann, *Front. Neurosci.* **2016**, *10*, 1.

[12] S. M. Potter, T. B. DeMarse, *J. Neurosci. Methods* **2001**, *110*, 17.

[13] M. Jorfi, J. L. Skousen, C. Weder, J. R. Capadona, *J. Neural Eng.* **2015**, *12*, 011001.

[14] P.-A. Mouthuy, S. J. Snelling, S. G. Dakin, L. Milković, A. Č. Gašparović, A. J. Carr, N. Žarković, *Biomaterials* **2016**, *109*, 55.

[15] T. Stieglitz, *Neuroethics* **2019**, DOI 10.1007/s12152-019-09406-7.

[16] S. Venkatraman, J. Hendricks, Z. A. King, A. J. Sereno, S. Richardson-Burns, D. Martin, J. M. Carmena, *IEEE Trans. Neural Syst. Rehabil. Eng.* **2011**, *19*, 307.

[17] A. Schander, T. Tesmann, S. Strokov, H. Stemmann, A. K. Kreiter, W. Lang, in *2016 38th Annu. Int. Conf. IEEE Eng. Med. Biol. Soc.*, IEEE, **2016**, pp. 6174–6177.

[18] X. T. Cui, D. D. Zhou, *IEEE Trans. Neural Syst. Rehabil. Eng.* **2007**, *15*, 502.

[19] C. Boehler, F. Oberueber, S. Schlabach, T. Stieglitz, M. Asplund, *ACS Appl. Mater. Interfaces* **2017**, *9*, 189.

[20] A. Lecomte, A. Degache, E. Descamps, L. Dahan, C. Bergaud, *Sensors Actuators B Chem.* **2017**, *251*, 1001.

[21] A. Schander, H. Stemmann, E. Tolstosheeva, R. Roese, V. Biefeld, L. Kempen, A. K.

Kreiter, W. Lang, *Sensors Actuators A Phys.* **2016**, *247*, 125.

[22] A. Schander, S. Strokov, H. Stemmann, T. Tebmann, A. K. Kreiter, W. Lang, *IEEE Sens. J.* **2019**, *19*, 820.

[23] M. Ganji, E. Kaestner, J. Hermiz, N. Rogers, A. Tanaka, D. Cleary, S. H. Lee, J. Snider, M. Halgren, G. R. Cosgrove, B. S. Carter, D. Barba, I. Uguz, G. G. Malliaras, S. S. Cash, V. Gilja, E. Halgren, S. A. Dayeh, *Adv. Funct. Mater.* **2018**, *28*, 1700232.

[24] Y. Lu, Y. Li, J. Pan, P. Wei, N. Liu, B. Wu, J. Cheng, C. Lu, L. Wang, *Biomaterials* **2012**, *33*, 378.

[25] I. Uguz, M. Ganji, A. Hama, A. Tanaka, S. Inal, A. Youssef, R. M. Owens, P. P. Quilichini, A. Ghestem, C. Bernard, S. A. Dayeh, G. G. Malliaras, *Adv. Healthc. Mater.* **2016**, *5*, 3094.

[26] D. W. L. Hukins, A. Mahomed, S. N. Kukureka, *Med. Eng. Phys.* **2008**, *30*, 1270.

[27] J. C. Barrese, N. Rao, K. Paroo, C. Triebwasser, C. Vargas-Irwin, L. Franquemont, J. P. Donoghue, *J. Neural Eng.* **2013**, *10*, 066014.

[28] J. P. Neto, P. Baião, G. Lopes, J. Frazão, J. Nogueira, E. Fortunato, P. Barquinha, A. R. Kampff, *Front. Neurosci.* **2018**, *12*, 270058.

[29] A. Lecomte, A. Degache, E. Descamps, L. Dahan, C. Bergaud, *Procedia Eng.* **2016**, *168*, 189.

[30] T. D. Y. Kozai, K. Catt, Z. Du, K. Na, O. Srivannavit, R. M. Haque, J. Seymour, K. D. Wise, E. Yoon, X. T. Cui, *IEEE Trans. Biomed. Eng.* **2016**, *63*, 111.

[31] D. A. Koutsouras, P. Gkoupidenis, C. Stolz, V. Subramanian, G. G. Malliaras, D. C. Martin, *ChemElectroChem* **2017**, *4*, 2321.

[32] M. Vomero, E. Castagnola, F. Ciarpella, E. Maggiolini, N. Goshi, E. Zucchini, S. Carli, L. Fadiga, S. Kassegne, D. Ricci, *Sci. Rep.* **2017**, *7*, 40332.

[33] A. S. Pranti, A. Schander, A. Bödecker, W. Lang, *Sensors Actuators B Chem.* **2018**, *275*, 382.

[34] V. F. Curto, B. Marchiori, A. Hama, A.-M. Pappa, M. P. Ferro, M. Braendlein, J. Rivnay, M. Fiocchi, G. G. Malliaras, M. Ramuz, R. M. Owens, *Microsystems Nanoeng.* **2017**, *3*, 17028.

[35] A. Håkansson, S. Han, S. Wang, J. Lu, S. Braun, M. Fahlman, M. Berggren, X. Crispin, S. Fabiano, *J. Polym. Sci. Part B Polym. Phys.* **2017**, *55*, 814.

[36] M. ElMahmoudy, S. Inal, A. Charrier, I. Uguz, G. G. Malliaras, S. Sanaur, *Macromol. Mater. Eng.* **2017**, *302*, 1600497.

Supporting Information

Stability of PEDOT:PSS-Coated Gold Electrodes in Cell Culture Media

*Gerwin Dijk[+] and Alexandra L. Rutz[+], George G. Malliaras**

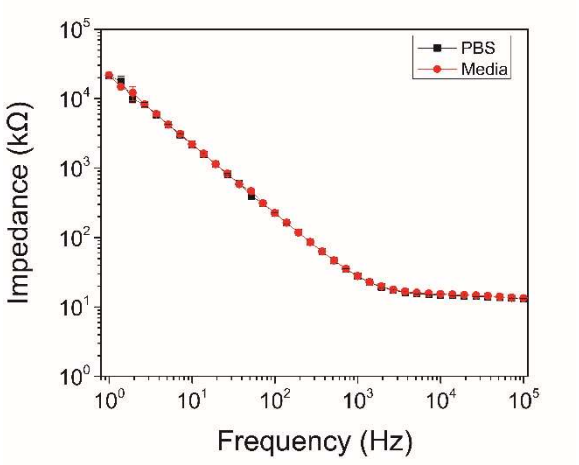

Figure S1. Comparison of impedance spectra for the same electrode in phosphate-buffered saline solution (PBS) and cell culture media.

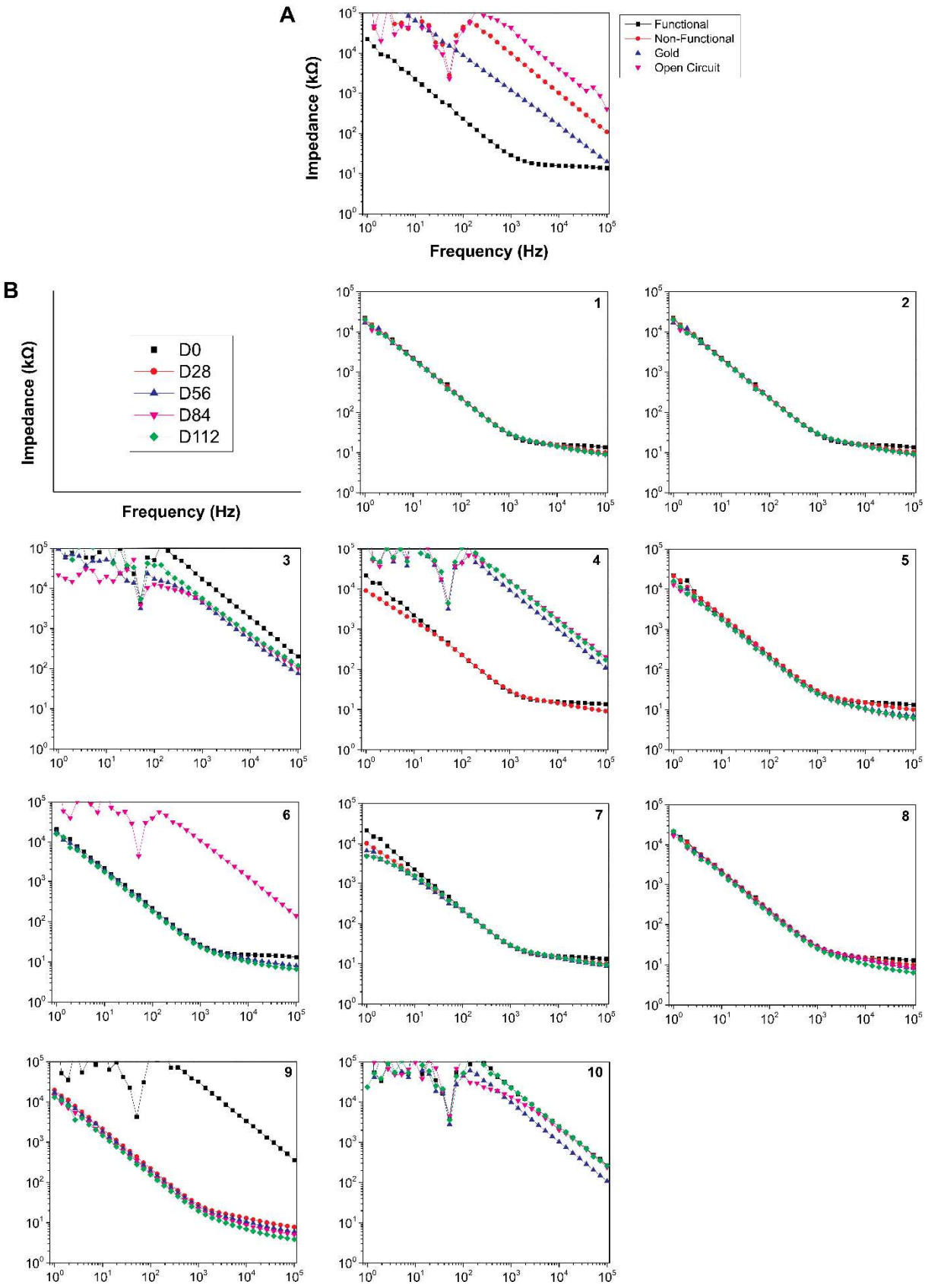

Figure S2. Impedance spectra of electrodes A) Representative functional (PEDOT:PSS-coated gold electrode) and non-functional electrodes, alongside a bare gold electrode and an impedance spectrum taken in an open circuit configuration (working electrode disconnected). Non-functional electrodes varied in impedance, but always had higher impedances above

1000 Hz than gold and always displayed erratic impedance below 100 Hz. B) an individual plot for each electrode. Impedance shown for day 0 and every month. Electrode number indicated in upper-right corner.

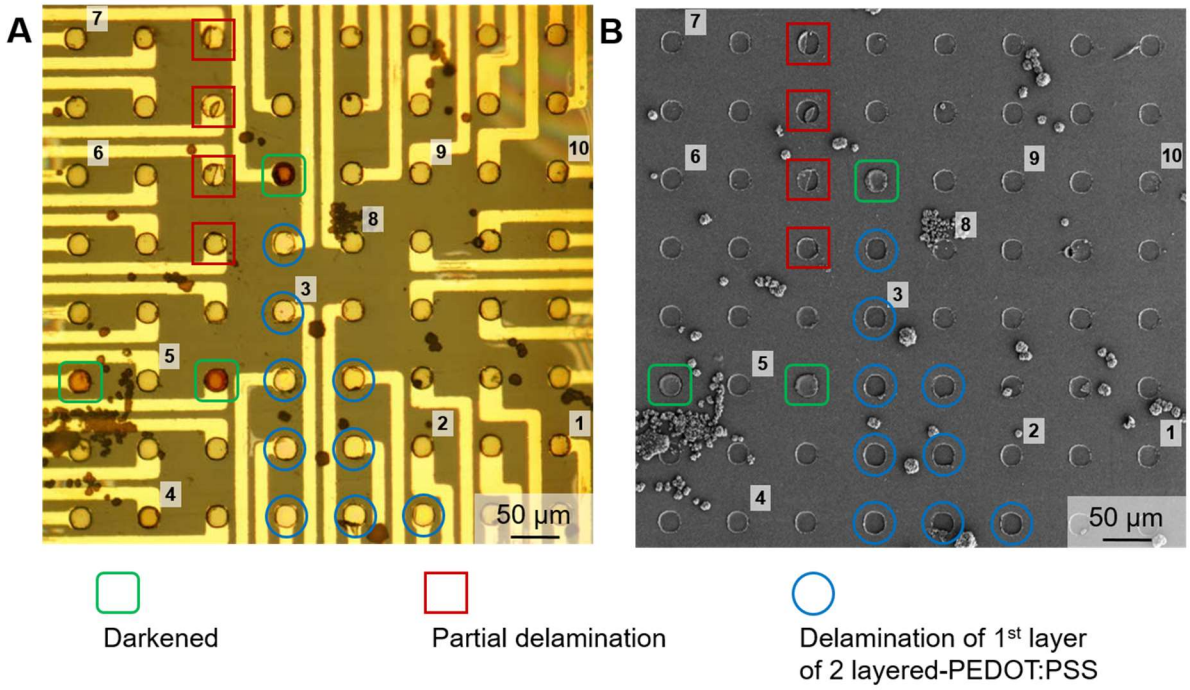

Figure S3. Light microscopy (A) and scanning electron microscopy (B) of the aged electrode array. Circular deposits appear to be crystalized salt. Monitored electrodes are numbered and electrodes that visually changed are indicated with symbols (key in figure).

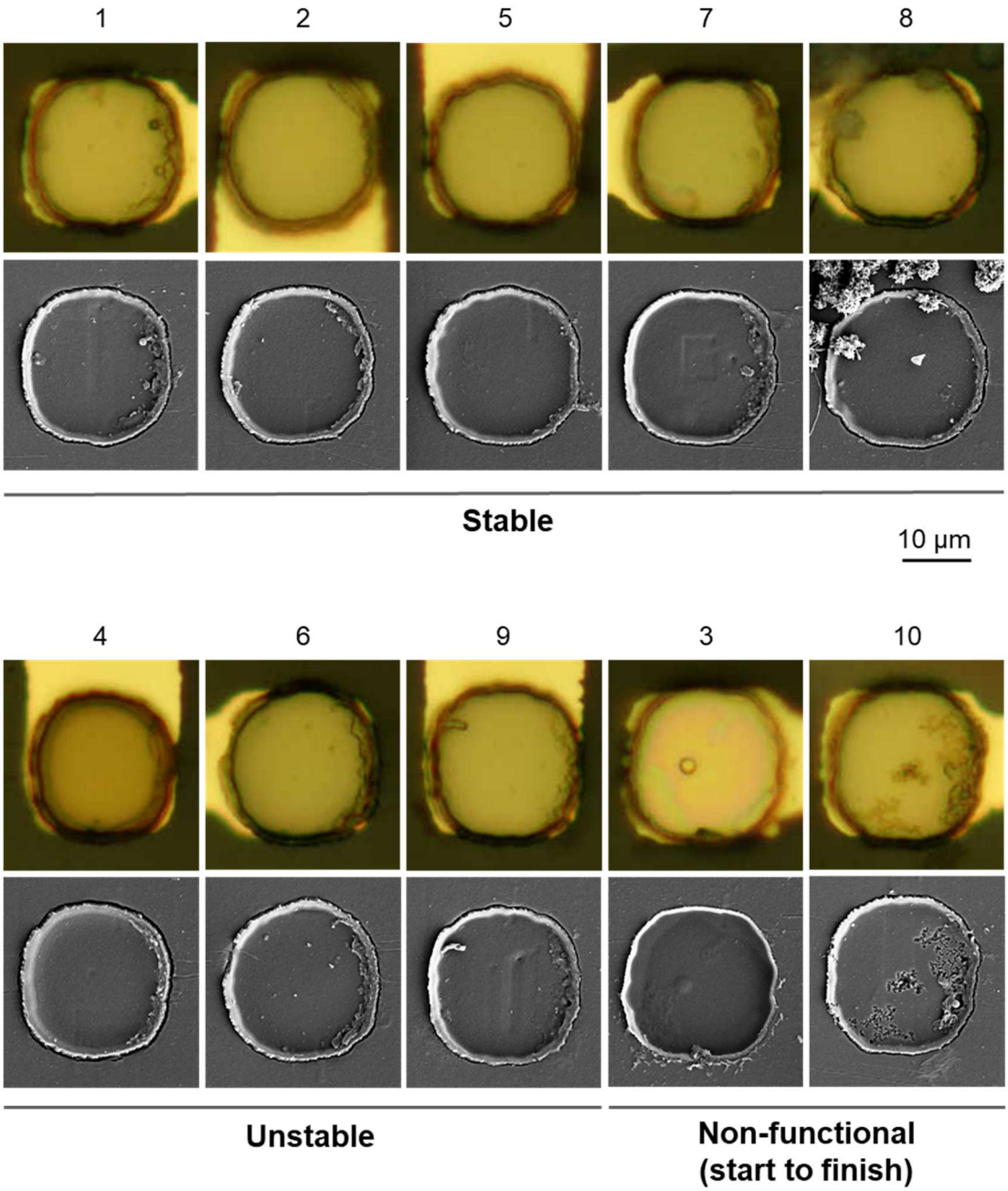

Figure S4. Light microscopy and scanning electron microscopy of the cultured electrodes categorized according to their functionality determined by EIS.

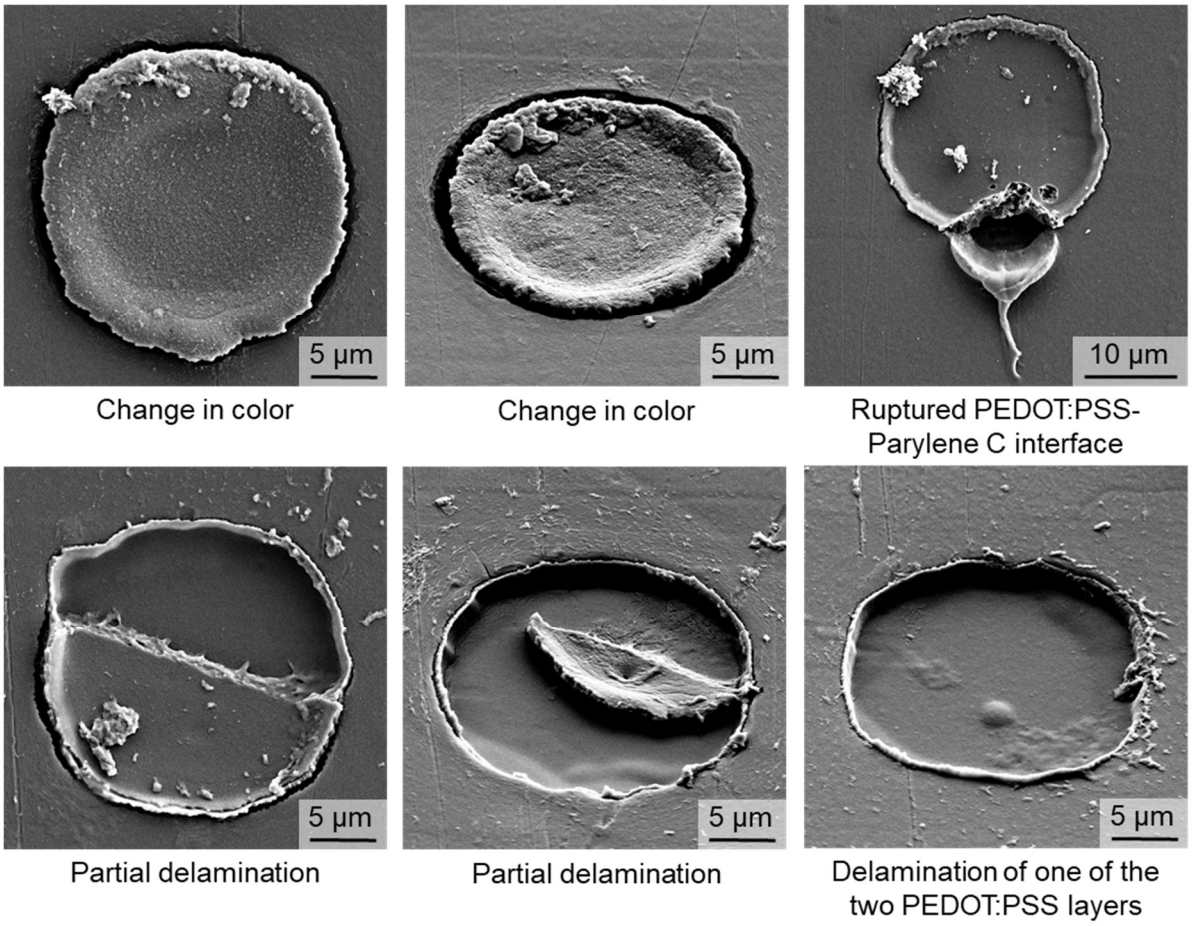

Figure S5. Additional scanning electron microscopy of electrodes with visual damage.